



## OPEN Alterations of the resting-state brain network connectivity and gray matter volume in patients with fibromyalgia in comparison to ankylosing spondylitis

Dong Liu<sup>1,3</sup>, Yanli Zhang<sup>1,3</sup>, Jiaoshi Zhao<sup>1</sup>, Budian Liu<sup>1</sup>, Churong Lin<sup>2</sup>, Mingcan Yang<sup>1</sup>, Jieruo Gu<sup>1</sup> & Ou Jin<sup>1</sup>

Fibromyalgia (FM) and ankylosing spondylitis (AS) are both rheumatic diseases characterized by significant musculoskeletal pain. In this study, we investigated the differences of the resting-state network (RSN) connectivity and gray matter volume (GMV) between FM, AS and healthy controls (HCs). We recruited 38 FM patients, 82 AS patients and 61 HCs in this study. All the participants underwent resting-state functional MRI (rs-fMRI) scans in a GE 3.0T MR system. Independent component analysis (ICA) was conducted on the rs-fMRI data, and group differences of the rsFC between different resting-state networks were calculated using dual regression. We also conducted voxel-based morphometry (VBM) analysis to investigate the differences of the GMV in FM, AS and HCs. The rsFC between the dorsal default mode network (DDMN) and the body of left caudate nucleus was significantly decreased in FM patients in comparison to AS patients (87 voxels,  $p = 0.025$ ). VBM analysis showed that the GMV of the left posterior lobe of cerebellum was significantly increased in FM patients compared with AS patients (88 voxels,  $p = 0.036$ ). Neither ICA nor VBM analysis revealed significant differences of RSN connectivity or GMV between FM patients and HCs. The altered rsFC between DMN and the caudate nucleus suggested an aberrant cortico-striato-thalamo-cortical circuit in FM patients, indicating aberrant reward processing, with potential association with mood, motivation and cognitive functions. The increased GMV in the left posterior lobe of cerebellum indicated the participation of cerebellum in the abnormal pain processing in FM patients.

**Keywords** Fibromyalgia, Ankylosing spondylitis, Functional connectivity, Functional MRI, Independent component analysis

### Abbreviations

FM	Fibromyalgia
AS	Ankylosing spondylitis
rs-fMRI	Resting-state functional magnetic resonance imaging
RSN	Resting-state network
BOLD	Blood oxygenation level-dependent
DMN	Default mode network
mPFC	Medial prefrontal cortex
PCC	Posterior cingulate cortex
MTG	Middle temporal gyrus
rsFC	Resting-state functional connectivity
ICA	Independent component analysis
HC	Healthy control
NSAIDs	Nonsteroidal anti-inflammatory drugs

<sup>1</sup>Department of Rheumatology, the Third Affiliated Hospital of Sun Yat-sen University, Guangzhou, China. <sup>2</sup>Department of Radiology, the Third Affiliated Hospital of Sun Yat-Sen University, Guangzhou, China. <sup>3</sup>Dong Liu and Yanli Zhang contributed equally to this work. ✉email: gujieruo@163.com; jinou@mail.sysu.edu.cn

VAS	Visual analogous scale
CRP	C reactive protein
FSS	Fatigue Severity Scale
BASDAI	Bath Ankylosing Spondylitis Disease Activity Index
bDMARD	Biological disease-modifying antirheumatic drugs
EPI	Echo planar imaging
FSL	FMRIB Software Library
FWHM	Full width at half maximum
MELODIC	Multivariate Exploratory Linear Decomposition into Independent Components
FIX	FMRIB's ICA-based Xnoiseifier
RMS	Root-mean squared
TFCE	Threshold-free cluster enhancement
FEW	Family error rate
ROI	Region of interest
VBM	Voxel-based morphometric
FPN	Fronto-parietal network
SN	Saliency network
DDMN	Dorsal DMN
L-FPN	Left FPN
R-FPN	Right FPN
GMV	Gray matter volume
OFC	Orbitofrontal cortex
CSTC	Cortico-striato-thalamo-cortical circuit
DS	Dorsal striatum
VS	Ventral striatum
MDD	Major depressive disorder
BDI	Beck Depression Inventory
CES-D	Center for Epidemiological Studies Scale

Fibromyalgia (FM) and ankylosing spondylitis (AS) are both rheumatic diseases characterized by significant musculoskeletal pain, with differences in etiology, pathogenesis and epidemiology<sup>1,2</sup>. Clinical manifestations of fibromyalgia include chronic widespread pain, often accompanied by fatigue, insomnia, depression and anxiety<sup>3</sup>, while ankylosing spondylitis is characterized by chronic lower back pain, sometimes with enthesitis, peripheral arthritis and dactylitis<sup>4</sup>. Although the pathogenic mechanism of fibromyalgia has not been fully elucidated, it has been proposed that central sensitization could largely explain the clinical features of FM patients<sup>5</sup>. Central sensitization refers to the malfunction of the neural circuits pertinent to the processing of afferent nociceptive stimuli, thereby causing increased sensitivity to noxious and non-noxious stimuli, namely allodynia and hyperalgesia<sup>6</sup>. On the other hand, the lower back pain in AS could be largely attributed to bona fide localized inflammation or structural changes at the axial skeleton<sup>7</sup>, while the neuropathic mechanism has also been reported to contribute to the perception of pain in AS<sup>8</sup>. According to real-world evidence, in female patients with ankylosing spondylitis 20.2% of misdiagnoses were fibromyalgia, which is significantly higher than male patients (6.6%)<sup>9</sup>. Such misdiagnoses are associated with longer diagnosis delay in AS patients. Due to the very different therapeutic strategies to the two disorders, it is important to differentiate FM from AS, especially in female patients, since inappropriate medication is not only ineffective, but also potentially detrimental<sup>10</sup>.

Resting-state functional magnetic resonance imaging (rs-fMRI) has enabled the evaluation of resting-state networks (RSNs) through the analysis of the blood oxygenation level-dependent (BOLD) signal, reflecting the spontaneous fluctuations of the brain connectivity<sup>11</sup>. It was believed that the aberrant connectivity and function of these RSNs might serve as the core feature to multiple psychiatric disorders and pain-related disorders<sup>12–14</sup>. Among the canonical RSNs, the default mode network (DMN) is the most widely studied. DMN plays a crucial role in the monitoring of internal mental landscape, with key nodes anchored to medial prefrontal cortex (mPFC), posterior cingulate cortex (PCC), precuneous, and middle temporal gyrus<sup>15,16</sup>. DMN is also sensitive to value judgment and social evaluation processes pertinent to self and others<sup>17</sup>. Previous research showed that the resting-state functional connectivity (rsFC) between DMN and insular cortex, as well as the right parahippocampal gyrus, was significantly increased in FM patients<sup>18,19</sup>, whereas the rsFC between DMN and the salience network was significantly increased in AS. However, there is no study directly comparing the RSN connectivity between the two diseases to identify potential neuroimaging markers specific to FM or AS.

Apart from the functional connectivity of the RSNs, voxel-based brain morphometric (VBM) studies have also revealed alterations of gray matter volume (GMV) of different brain areas in AS and FM. VBM studies in AS showed increased gray matter volume in the thalamus and putamen<sup>20,21</sup>, as well as cortical thinning in the primary somatosensory, insular, anterior cingulate, anterior mid-cingulate cortices and the supplemental motor area<sup>20</sup>. Alterations of GMV is extensively studied in FM, and these studies consistently reported decreased GMV in anterior cingulate and paracingulate cortices, posterior cingulate and paracingulate cortices, and parahippocampal gyrus<sup>22–25</sup>, while increased GMV is consistently seen in the left cerebellum<sup>25</sup>. However, there is also no study directly comparing the GMV of different brain areas between AS and FM.

In this study, we aimed to investigate the differences of the rsFC of the RSNs as well as the alterations of GMV between AS and FM. We utilized the independent component analysis (ICA) approach, which is a data-driven method calculating the temporal covariance of different brain areas, thus reducing bias commonly seen in hypothesis-driven methods such as seed-based connectivity analysis<sup>26,27</sup>. We also performed VBM analysis using FSL's FSL-VBM<sup>28</sup>. We hypothesized that DMN would exhibit altered connectivity with other brain areas,

potentially the insular network or the salience network relative to FM or AS, and that VBM analysis would show significantly altered GMV in certain brain areas. By investigating the differences of RSN connectivity and GMV between AS and FM, we could further understand the distinct pathophysiological mechanisms underlying the perception of pain in the two diseases, and seek neuroimaging markers that could potentially differentiate AS from FM.

## Methods

### Subjects

Three independent cohorts were assessed in this study. The FM cohort consisted of 41 FM patients who visited the rheumatology clinic of the Third Affiliated Hospital of Sun Yat-sen University. Patients in this cohort were recruited if they were diagnosed as fibromyalgia based on the American College of Rheumatology Diagnostic Criteria for Fibromyalgia<sup>29</sup>. The AS cohort and healthy control (HC) cohort was derived from another ongoing neuroimaging study investigating the group differences of large-scale networks between AS patients and HC. The inclusion criteria of the AS cohort included: (1) fulfilling the 1984 Modified New York Criteria for the diagnosis of ankylosing spondylitis based on radiographs<sup>30</sup>; (2) having an average back pain score  $\geq 1$  (on a 0–10 scale); (3) did not receive biologics treatment in the past two months, including TNF- $\alpha$  inhibitors and IL-17 inhibitors. Patients of the FM or AS cohort were allowed to remain on stable preventative or as-needed medication (NSAIDs). Exclusion criteria of the HC cohort were conditions associated with pain (migraine, dysmenorrhea) or having taken any pain medication other than NSAIDs within one month of the scan or for more than one month within the last 6 months.

This study was approved by the Research Ethics Board of the Third Affiliated Hospital of Sun Yat-sen University. Written informed consent was obtained from patients prior to the inclusion of this study according to the Declaration of Helsinki.

### Clinical assessment

For the subjects in the FM cohort and the AS cohort in this study, clinical information including age, sex and disease duration were collected in the form of questionnaire. Current pain at the time of the fMRI scan was assessed using the visual analogue scale (VAS), recorded on a 0–10 rating scale (0 = no pain, 1 = pain threshold, 10 = worst bearable pain). Global pain of the past week was also recorded. In the FM cohort, the extent of widespread pain and its severity were quantified with widespread pain index (WPI) and symptom severity scale (SSS)<sup>29</sup>. Moreover, sleep quality was assessed using Pittsburgh sleep quality index (PSQI)<sup>31</sup>, while anxiety and depression was evaluated using hospital anxiety and depression scale (HADS)<sup>32</sup>. Laboratory results including C reactive protein (CRP), HLA-B27 positivity were retrieved. For the AS cohort, severity of fatigue was assessed using the modified 9-item, 10-point Fatigue Severity Scale (FSS)<sup>33</sup>, while the disease activity was assessed using Bath Ankylosing Spondylitis Disease Activity Index (BASDAI)<sup>34</sup>. Previous medication, including NSAIDs, bDMARDs, corticosteroids, duloxetine, pregabalin and sedatives, was recorded according to the medical history.

### MRI session

All subjects underwent MRI of the brain on a 3.0-Tesla MR system (Discovery MR750, General Electric, Milwaukee, WI) with an 8-channel phased-array head coil. Each participant was required to lie quietly in the supine posture with eyes open without falling asleep, and head movement was reduced to the minimum by using foam padding around (outside of) the head. Structural and functional MRI data were acquired during a single session. Structural (3D T1-weighted) MRI data were acquired using a 3D BRAVO sequence (flip angle = 9°, TR = 6.6 ms, TE = 2.5 ms, matrix size = 256 × 256, slice thickness = 1 mm, number of slices = 176, time of acquisition: 3:50 min). And resting-state fMRI data were acquired using a BOLD protocol with a T2\*-weighted gradient echo planar imaging (EPI) sequence (flip angle = 90°, TR = 2000 ms, TE = 30 ms, matrix size = 192 × 192, slice thickness = 3 mm, number of slices = 41, 240 dynamics, time of acquisition: 8 min). All images underwent strict quality inspection by a rheumatologist and a radiologist.

### MRI data preprocessing and analysis

#### *Resting state fMRI preprocessing*

The preprocessing of the MRI images was conducted using FMRIB Software Library (FSL, version 6.0.7.6). Brain extraction was performed using the Brain Extraction Tool multiple-iteration method. The first 10 volumes of the functional images were removed to ensure signal stabilization, followed by head motion correction by volume-realignment to the middle volume using MCFLIRT<sup>35</sup>. Images were smoothed with a Gaussian kernel of 5 mm full width at half maximum (FWHM). MELODIC (Multivariate Exploratory Linear Decomposition into Independent Components) (version 3.14) was employed to conduct the single-session probabilistic independent component analysis of rs-fMRI data<sup>36</sup>. We used FMRIB's ICA-based Xnoisefer (FIX 1.06.15) to automatically detect and remove artifacts from each single-session probabilistic ICA data<sup>37</sup>. The "Standard.RData" training dataset provided by the FIX toolbox was used to classify the components conforming to motion artifacts, white matter or cerebrospinal fluids signal or other artifacts caused by MRI acquisition-related issues based on the spatial map and the time series (classification threshold = 20). We randomly selected the classification results of the FIX procedure and compare the results with manual inspection, and it was confirmed that the artifactual components recognized by FIX were correctly classified. The denoised rs-fMRI images were high-pass filtered at 0.01 Hz, then registered to the high-resolution T1-weighted images using boundary-based registration in FLIRT, and subsequently to the MNI space using 12-parameter affine transformation and non-linear registration in FNIRT. The denoised and registered functional images were used in further analysis of functional connectivity.

### ICA functional connectivity

The denoised and registered functional images were temporally concatenated to generate a 4-dimensional dataset. We used MELODIC in FSL to decompose the generated 4-dimensional dataset into 25 components through group ICA process<sup>36</sup>. The spatial maps of each component were manually inspected and classified as resting-state networks based on the spatial distribution patterns of the networks. The RSNs were compared to the canonical large-scale networks proposed by Smith et al<sup>38</sup>, and we could identify twelve canonical networks in our study. During the first stage of dual regression, the spatial maps of the full set of the 25 components were used as the spatial regressors to extract the time series from the voxels within the region of each subject. In the second stage, the extracted time series were regressed against the rs-fMRI data of each subject so as to generate the subject-specific spatial maps corresponding to the components.

In the general linear model, we included age and sex as regressors of no interest in the voxel-wise two-sample unpaired t-test on the subject-specific spatial maps corresponding to each component, since the age and sex were significantly different between FM patients and AS patients<sup>1,2</sup>. We calculated the group differences of rsFC of the RSNs between FM and AS, as well as between FM and HC. Significant differences between groups were determined using FSL's randomise (permutation tests). All tests were fully corrected for multiple comparisons across voxels using FSL's threshold-free cluster enhancement (TFCE) and a family error rate (FWE) of  $p$  smaller than 0.05.

### Correlation between rsFC of RSNs and clinical characteristics of FM patients

To investigate the association between the altered rsFC of the RSNs and the clinical characteristics of the FM patients, we first conducted Pearson correlation analysis in a region of interest (ROI)-wise manner. The ROI was defined as the region with significantly altered rsFC with the RSNs in FM patients. We created masks based on the shapes of the ROIs and extracted the average rsFC z values in the corresponding regions. We calculated the Pearson correlation coefficients between the average extracted rsFC z values and age, disease duration, current VAS, global pain, FSS, WPI, SSS, PSQI, HADS-Anxiety, HADS-Depression of the FM patients.  $P$ -values < 0.005 (with Bonferroni correction for multiple comparisons) were considered statistically significant.

We further conducted separate voxel-wise regression analysis of the RSNs on the whole brain level, searching for regions with rsFC significantly correlated with the clinical characteristics of FM patients. Results of the voxel-wise regression analysis were considered significant at  $p < 0.005$  (with Bonferroni correction for multiple comparisons).

### Voxel-based morphometric analysis

We conducted the voxel-based morphometric analysis using FSL's FSL-VBM<sup>28</sup>. Using the structural images as reference, we extracted the brain with Brain Extraction Tool. Subsequently, the gray matter was segmented, followed by registration to the MNI152 standard space with non-linear registration method. The preprocessed structural images were averaged and flipped along the x-axis to create a symmetric gray matter template. The gray matter image of each participant was registered to this template also using non-linear registration and modulated to correct for local expansion in light of the non-linear component of the spatial transformation. The modulated gray matter images were then smoothed with an isotropic Gaussian kernel with a sigma of 3 mm, followed by voxel-wise GLM using non-parametric testing with 5,000 permutations, correcting for multiple comparisons across space. The total intracranial volume (TIV) of each participant was calculated using Computational Anatomy Toolbox (CAT12)<sup>20</sup>. We calculated the group differences of gray matter volume between different groups, by including age, sex and TIV as covariates of no interest.

## Results

### Demographic and clinical characteristics

Due to excessive head motion (absolute RMS displacement > 2 mm or relative RMS displacement > 0.4 mm), 1 FM patient, 3 AS patients and 2 HC were excluded from this study. ANOVA results showed that there was no significant difference in the absolute RMS displacement ( $p = 0.719$ ) or the relative RMS displacement ( $p = 0.267$ ) among the three cohorts. Due to missing volumes or different MRI scanning protocol, 2 FM patients, 3 AS patients and 1 HC were also excluded. A total of 38 FM patients, 82 AS patients and 61 HC were included in the final analysis. The demographic and clinical measures were presented in Table 1.

### Recognition of RSNs

Corresponding to the canonical networks proposed by Smith et al<sup>38</sup>, we could identify 12 RSNs from the 25 components generated from the group ICA calculations. The 12 RSNs included DMN, fronto-parietal network (FPN), salience network (SN), cingulo-opercular network, auditory sensorimotor network, visual networks, and cerebellar networks. The DMN was decomposed into ventral and dorsal DMN (DDMN), while the FPN was decomposed into left and right FPN (L-FPN and R-FPN), which is very common in previous neuroimaging studies<sup>39,40</sup>. The cerebellar network was split into the upper part and lower part. Besides the 12 canonical RSNs, we could also recognize RSNs anchored to the orbital-frontal cortex, the basal ganglia or the pons, but these RSNs were not included in the further analysis. The rest of the RSNs corresponded to the signals of the third or the fourth ventricle, or were derived from motion artifacts. Figure 1 presents the 12 canonical RSNs identified in this study.

### Altered rsFC of RSNs

Compared with AS patients, the rsFC between dorsal DMN and a cluster located at the left caudate nucleus was significant decreased in FM patients. (Figures 2 and 87 voxels,  $p = 0.025$ , TFCE-corrected for multiple

	AS (n = 82)	FM (n = 38)	HC (n = 61)
Age (years)	31.67 ± 10.00	38.97 ± 11.68	31.44 ± 7.35
Male/female	57/25	11/27	37/24
Disease duration (years)	5 [2–12]	1.75 [0.5–5]	/
Current VAS (0–10)	3 [2–5.25]	4.5 [3–6]	/
Global pain (0–10)	4.5 [2.5–6]	6 [4–8]	/
FSS score	3.94 ± 2.49	3.98 ± 1.12	/
WPI	/	9.17 ± 2.12	/
SSS	/	7.31 ± 1.69	/
HADS-anxiety	/	9.14 ± 3.56	/
HADS-depression	/	8.26 ± 3.12	/
BASDAI	3.24 ± 1.84	/	/
CRP	6.3 [1.3–28.15]	0.8 [0.35–1.4]	/
HLA-B27 positivity	74/82 (91.5%)	2/38 (5.3%)	
Medication			
NSAIDs	51/82 (62.2%)	22/38 (57.9%)	/
bDMARDs	31/82 (37.8%)	/	/
Corticosteroids	1/82 (1.2%)	/	/
Duloxetine	/	15/38 (39.5%)	/
Pregabalin	/	15/38 (39.5%)	/

**Table 1.** Demographic and clinical characteristics of AS patients, FM patients and HCs. AS, ankylosing spondylitis; FM, fibromyalgia; HC, healthy control; VAS, visual, analogous scale; FSS, fatigue severity scale; WPI, widespread pain index; SSS, symptom severity scale; HADS, Hospital anxiety and depression scale; BASDAI, Bath Ankylosing Spondylitis Disease Activity Index; CRP, C-reactive protein; NSAIDs, nonsteroidal anti-inflammatory drugs; bDMARDs, biological disease-modifying antirheumatic drugs. Values represent mean ± SD (normal distribution), median [interquartile range] (skewed distribution) or n (% of total).

comparisons) The characteristics of this cluster could be seen in Table 2. We could not identify any cluster with significantly increased rsFC with the RSNs in FM patients compared with AS patients.

We could not find any cluster with significantly altered rsFC of the RSNs between FM patients and HC.

### Correlation between rsFC of RSNs and clinical characteristics of FM patients

We investigated whether the rsFC between DDMN and left caudate nucleus was correlated with the clinical characteristics of the FM patients, including age, disease duration, current VAS, global pain, FSS, WPI, SSS, PSQI, HADS-Anxiety, HADS-Depression. There was no correlation between the rsFC and these clinical characteristics of FM patients. (Supplementary Figs. 1–10)

Voxel-wise regression analysis on the whole-brain level showed that the rsFC within the FPN was significantly disturbed as the age of FM patients increased. We identified two clusters within the left FPN with rsFC inversely correlated with the age of FM patients. (Table 3; Fig. 3A and B; Cluster 1: 1,179 voxels,  $r = -0.75$ ,  $p < 0.001$ ; Cluster 2: 728 voxels,  $r = -0.76$ ,  $p < 0.001$ . Both were TFCE-corrected for multiple comparisons.) We also found a cluster within the right FPN with rsFC inversely correlated with the age of FM patients. (Table 3; Figs. 3C and 706 voxels,  $r = -0.7$ ,  $p < 0.001$ , TFCE-corrected for multiple comparisons)

### Voxel-based morphometric analysis

Results of the VBM analysis showed that the GMV of the left posterior lobe of cerebellum is significantly increased in FM patients, in comparison with AS patients. (Fig. 4; Tables 4 and 88 voxels,  $p = 0.036$ , TFCE-corrected for multiple comparisons)

In comparison with the HCs, we could not find any cluster with significantly increased or decreased GMV in FM patients.

## Discussion

This study directly compared the rsFC of the large-scale networks between FM patients and AS patients, utilizing the data-driven ICA approach. Results showed that FM patients exhibited significantly decreased rsFC between DDMN and the body of the right caudate nucleus, suggesting a disturbance of the cortico-striato-thalamo-cortical circuit (CSTC). Moreover, the GMV of the bilateral posterior cerebellum of FM patients was significantly decreased compared to HC, while a small cluster in right OFC also showed significantly decreased GMV in FM patients.

Recent research suggested that besides being a sensorimotor structure, the basal ganglia is also involved in the elements leading to action, including emotion, motivation, and cognition<sup>41</sup>. The basal ganglia consists of the dorsal striatum (DS) and ventral striatum (VS). DS is comprised of the caudate nucleus and the putamen, while the nucleus accumbens, along with the rostroventral-most aspects of the caudate nucleus and the putamen,



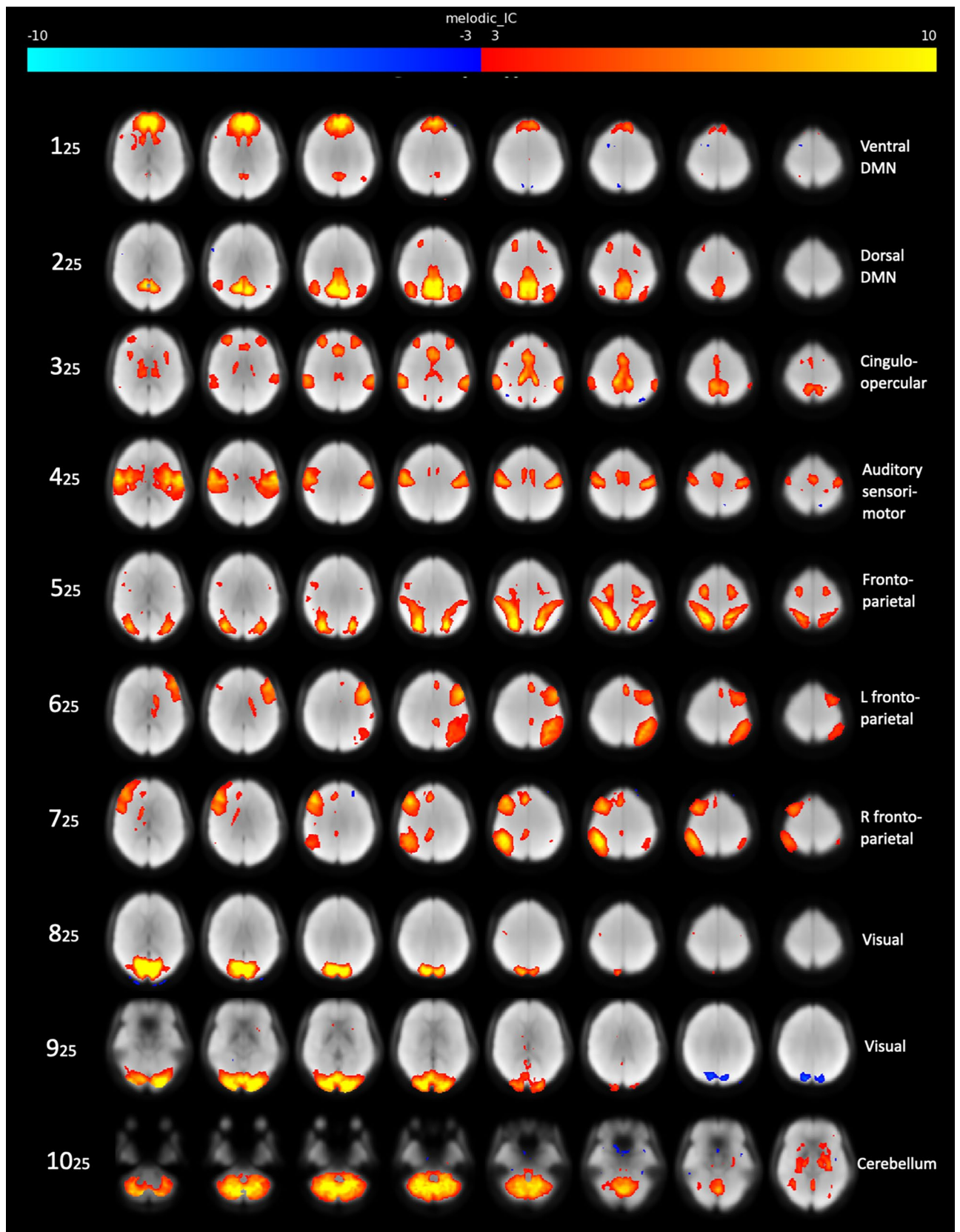


**Fig. 1.** RSNs identified in the independent component analysis of FM patients, AS patients and HCs. Brain images are presented in radiological convention (Left hemisphere appears on the on the right side of the brain). RSN, resting-state network; FM, fibromyalgia; AS, ankylosing spondylitis; HC, healthy control; DMN, default mode network; L, left; R, right.

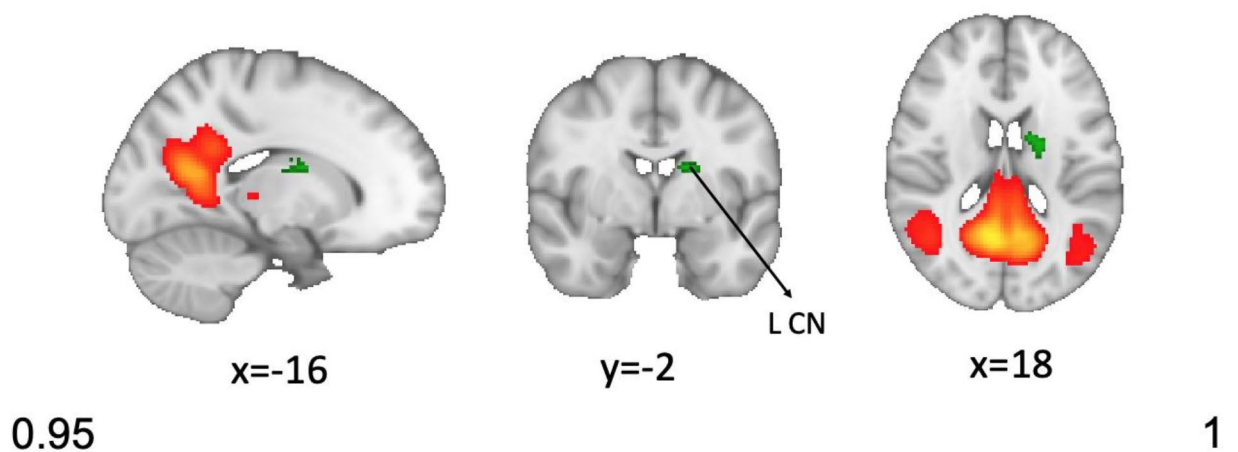


**Fig. 2.** Region of altered rsFC between FM patients and AS patients. The rsFC between DDMN (red) and the body of the left caudate nucleus (green) is significantly decreased in FM patients in comparison with AS patients, controlling for age and sex. (Cluster-level  $P$  (TFCE corr.) = 0.025) Brain images are presented on MNI standard brain, showing regions with cluster-level TFCE-corrected  $p$  value < 0.05. rsFC, resting-state functional connectivity; FM, fibromyalgia; AS, ankylosing spondylitis; DDMN, dorsal default mode network; L CN, left caudate nucleus; TFCE, threshold-free cluster enhancement.

Connectivity	Number of voxels	X (mm)	Y (mm)	Z (mm)	Cluster-level $P_{TFCEcorr}$
AS > FM (controlling for age and sex)					
DDMN	87	-16	-2	18	0.025

**Table 2.** Region of altered rsFC in FM patients compared with AS patients. The X, Y, Z represent the peak MNI coordinates. AS, ankylosing spondylitis; FM, fibromyalgia; DDMN, dorsal default mode network; FWE, family-wise error.

Connectivity	Number of voxels	X (mm)	Y (mm)	Z (mm)	$r$	$P$ -value
Age						
L-FPN	1,179	-32	-48	39	-0.75	<0.001
L-FPN	728	-50	-60	2	-0.76	<0.001
R-FPN	2,706	49	25	9	-0.7	<0.001

**Table 3.** Regions of rsFC correlated with age and the corresponding Pearson correlation coefficient in FM patients. The X, Y, Z represent the peak MNI coordinates. L, left; R, right; FPN, frontoparietal network; FM, fibromyalgia.

form the VS<sup>41</sup>. The caudate nucleus could be functionally divided into three parts, including limbic, associative and sensorimotor areas<sup>42</sup>. The rostroventral-most part of the caudate nucleus receives input from the limbic and paralimbic cortices, while the associative area comprised most of the caudate nucleus, with fiber connections with the frontal, parietal and temporal lobes. Additionally, the sensorimotor area is anchored to the dorsolateral edge of the head of the caudate nucleus, receiving input from the primary motor and sensorimotor cortices<sup>43</sup>. Output of the basal ganglia is transmitted to the cerebral cortex (mostly the frontal cortex) via the thalamus, thus forming the CSTC<sup>41,43</sup>.

In the current study, the rsFC between DMN and the body of the caudate nucleus was significantly decreased in FM patients in comparison to AS patients. Previous studies have confirmed that corticostriatal connectivity underlies reward processing in major depressive disorder (MDD)<sup>44</sup>, since the caudate nucleus contributed to behavior through the excitation of correct action schemas based on the evaluation of action-outcomes, as opposed to the stimulus-response function by the putamen<sup>42</sup>. MDD patients showed blunted activation of the caudate nucleus when presented with monetary gains, while the GMV of the caudate nucleus was inversely correlated with anhedonia in MDD patients<sup>44,45</sup>. Another study showed that patients in early stages of depression seeking for treatment had deficits in DMN connectivity with the caudate nucleus<sup>46</sup>. Based on the association

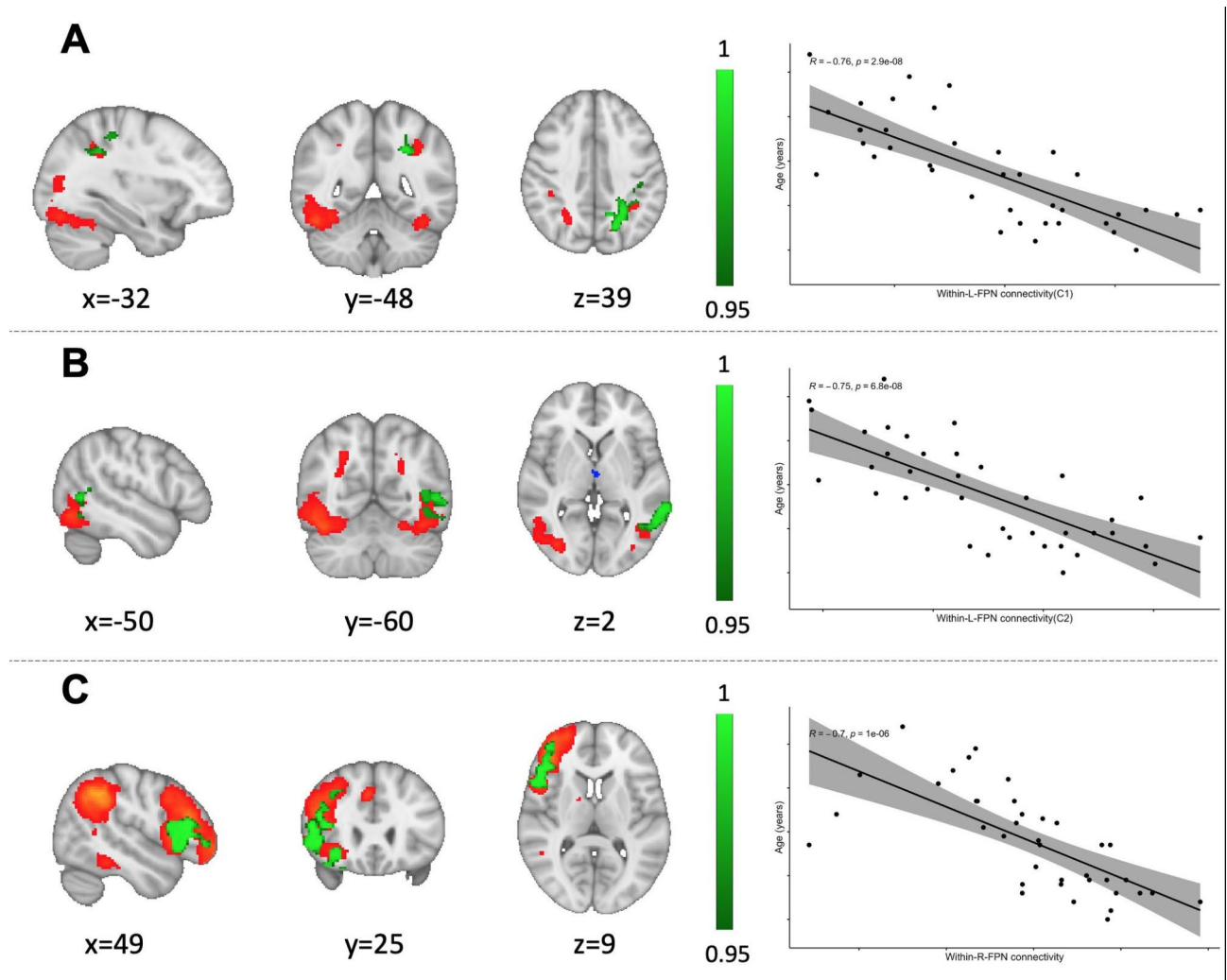


**Fig. 3.** Regions of rsFC correlated with the age of FM patients identified in voxel-wise regression analysis. The scatter plots show the mean connectivity between this cluster and the corresponding RSN for each FM patient plotted against their age. **(A)** The first cluster (green) within the L-FPN (red) showing rsFC anticorrelated with age ( $r = -0.75$ ,  $p < 0.001$ ). **(B)** The second cluster (green) within the L-FPN (red) showing rsFC anticorrelated with age ( $r = -0.76$ ,  $p < 0.001$ ). **(C)** One cluster (green) within the R-FPN (red) with rsFC inversely correlated with age ( $r = -0.7$ ,  $p < 0.001$ ). Regions are presented on MNI standard brain. rsFC, resting-state functional connectivity; FM, fibromyalgia; RSN, resting-state network; L, left; R, right; C1, cluster 1; C2, cluster 2.

between DMN-caudate nucleus connectivity and reward processing, the decreased DMN-caudate nucleus rsFC in FM patients might indicate the presence of mood disorders such as depression and anxiety. This is also in line with our understanding of FM, that stress and depression play a crucial role in the pathophysiology of FM<sup>47</sup>. FM patients showed statistically significant differences in the measures such as depression measures, Beck Depression Inventory (BDI) and Center for Epidemiological Studies Scale (CES-D)<sup>22,48</sup>. Moreover, FM patients often present other psychosomatic symptoms, including sleep disturbances, fatigue and cognitive dysfunction<sup>2</sup>. Previous studies showed that mind-body therapies such as meditation could achieve pain relief through the involvement of caudate nucleus<sup>49</sup>, and it could be speculated that mind-body therapies could achieve alleviation of pain in FM patients through adjusting the CSTC connectivity. Clinical trials are needed to examine the role of CSTC connectivity in the therapeutic effects of mind-body therapy in FM patients. However, in the correlation analysis, we could not establish the correlation between the altered rsFC and these clinical characteristics. It should be noted that although the rsFC was not linearly correlated with the clinical measures, it could still indicate that rsFC could be an intrinsic trait to the disease per se. More research is required to verify this association between the altered DMN-caudate nucleus rsFC and the clinical characteristics of fibromyalgia.

Another interesting finding is that age, rather than disease duration, was inversely correlated with the within-FPN connectivity in FM patients. This is not unexpected since previous studies reported that older adults showed reduced functional connectivity within the FPN<sup>50–52</sup>. In contrast to DMN, which monitors the internal mind landscape and self-referential thoughts, FPN is considered essential for actively maintaining and manipulating



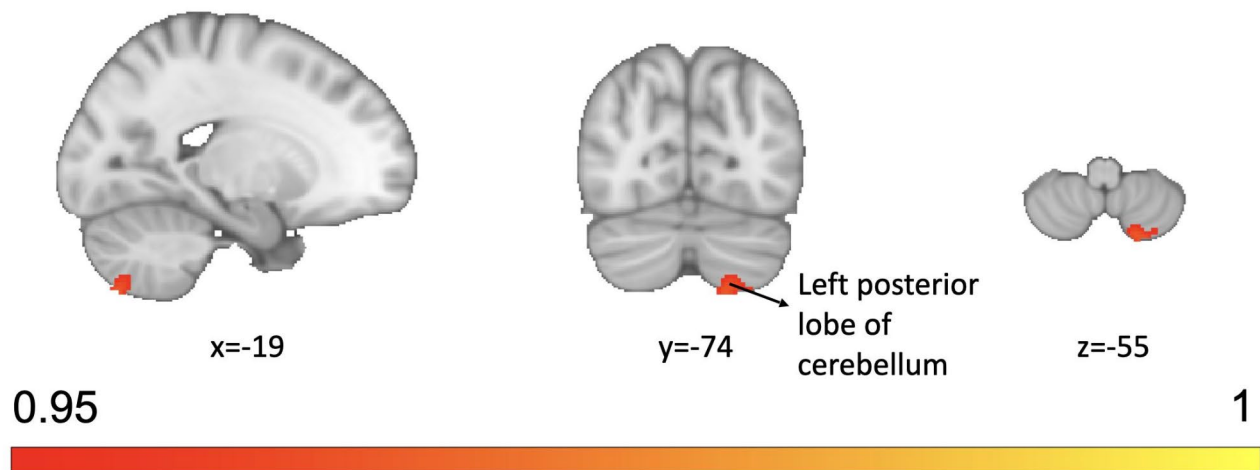


**Fig. 4.** Region of significantly altered GMV in FM patients in comparison with AS patients. The GMV of the left posterior lobe of the cerebellum (red) is significantly increased in FM patients in comparison with AS patients. (Cluster-level  $P$  (TFCE corr.) = 0.036) Brain images are presented on MNI standard brain, showing regions with cluster-level TFCE-corrected  $p$  value  $< 0.05$ . GMV, gray matter volume; FM, fibromyalgia; AS, ankylosing spondylitis; TFCE, threshold-free cluster enhancement.

Location	Number of voxels	X (mm)	Y (mm)	Z (mm)	Cluster-level $P_{TFCEcorr}$
FM > AS					
Left posterior lobe of Cerebellum	88	-19	-74	-55	0.036

**Table 4.** Regions with altered GMV in FM patients in comparison with AS patients. The X, Y, Z represent the peak MNI coordinates. GMV, gray matter volume; FM, fibromyalgia; AS, ankylosing spondylitis.

information in working memory, as well as decision-making in goal-directed behavior<sup>15,17</sup>. Disruption of the intra-network connectivity of the FPN suggests greater distractibility and poorer problem-solving capability<sup>51</sup>.

VBM results showed that the GMV of the left posterior lobe of the cerebellum was significantly increased in FM patients in comparison to AS patients. This finding is in line with previous studies, consistently reporting that the GMV of the left cerebellum is significantly increased in FM compared with HCs<sup>22–24</sup>. A meta-analysis aggregated 7 VBM studies on FM and concluded that regional GMV increases were consistently found in the left cerebellum<sup>25</sup>. Moreover, local increase of GMV at the cerebellum was positively correlated with psychological stress in FM patients<sup>53</sup>. Although the cerebellum is rarely perceived as a pain-processing area, accumulating evidence suggested that the cerebellum might be implicated in the nociception and chronic pain syndromes. Lobules IV–VI and Crus I of the cerebellum are especially pertinent to pain processing, since acute pain consistently evoked signal intensity increases in these areas, while chronic pain was also consistently reported to be associated with altered activation strength under noxious stimuli in lobules V–VI and Crus I<sup>54,55</sup>. Moreover, multiple studies have also revealed the abnormal integration between cerebellum and other brain areas. In adolescents with new daily persistent headaches, the connectivity between Crus II of cerebellum and the frontal and parietal cortices was significantly increased<sup>56</sup>. In contrast, the rsFC between the right lobule V as well as bilateral Crus I and the default mode network as well as the salience network is significantly decreased in chronic lower back pain<sup>57</sup>. Kim et al. reported dense cerebellar connections with medial prefrontal/orbitofrontal cortex, medial temporal lobe and right inferior parietal lobule, and that the number of white matter fibers were associated with greater evoked pain sensitivity and clinical pain inference<sup>22</sup>. All the evidence above suggested that cerebellum plays an important role in the nociceptive processing in FM patients, and that it should be given more attention in future research.

A peculiar observation is that although existing literature reported a number of differences in the rsFC and GMV between FM patients and HCs<sup>18,19,22,23,25</sup>, none of the results were replicated in the current study. Only the significantly increased GMV in the left posterior lobe of the cerebellum were shown in FM patients in comparison with AS patients. This discrepancy could be mainly attributed to the statistical power, since the sample size in the AS cohort is bigger than the HC cohort. Another factor could be the demographic characteristics of the HC cohort. Although we included the age and sex as covariates of no interest, this discrepancy could still result in the absence of statistical difference.

There are a few limitations to this study. The foremost limitation is that this study was a cross-sectional study, and we could not establish the causal relationship between the disease condition and the altered brain connectivity. We intend to conduct longitudinal studies in the future to examine whether there is a causal

relationship between brain connectivity changes and the progression of FM. Second, FM is a common comorbidity of AS, and earlier reports showed that the prevalence of fibromyalgia in AS patients was 13.8%<sup>58</sup>. The AS cohort in this study was derived from another independent neuroimaging study, and its study protocol did not evaluate the comorbidity of fibromyalgia. Therefore, we could not stratify the AS patients based on their comorbidity status of fibromyalgia, which might confound the results. In the future we will exclude patients with comorbidity of FM to verify whether the alteration discovered in our study is specific to FM. Third, since medication such as duloxetine and pregabalin might have an impact on the functional connectivity, it would be more appropriate to include the medication use as covariates of no interests. Future work is needed to determine to what extent the medication use has an impact on the altered rsFC.

## Conclusion

We found that the DMN-caudate nucleus connectivity was significantly decreased in FM patients in comparison to AS patients. This finding indicated an aberrant CSTC circuit and its effect on the reward processing might be compromised, with potential association with altered emotion, motivation and cognitive functions in FM. The significantly increased GMV in the left posterior lobe of the cerebellum indicated that the cerebellum might be implicated in the abnormal nociceptive processing in FM, thereby causing allodynia and hyperalgesia. Future research is required to verify these alterations as reliable neuroimaging biomarkers to differentiate FM from AS.

## Data availability

The datasets used and/or analysed during the current study are available from the corresponding author on reasonable request.

Received: 7 August 2024; Accepted: 7 November 2024

Published online: 02 December 2024

## References

1. Clauw, D. J. Fibromyalgia: a clinical review. *JAMA*. **311** (15), 1547–1555 (2014).
2. Taurog, J. D., Chhabra, A. & Colbert, R. A. Ankylosing spondylitis and Axial Spondyloarthritis. *N Engl. J. Med.* **374** (26), 2563–2574 (2016).
3. Bair, M. J., Krebs, E. E. & Fibromyalgia *Ann. Intern. Med.* ;**172**(5), ITC33–ITC48 (2020).
4. Sieper, J. & Poddubnyy, D. Axial spondyloarthritis. *Lancet*. **390** (10089), 73–84 (2017).
5. Cagnie, B. et al. Central sensitization in fibromyalgia? A systematic review on structural and functional brain MRI. *Semin Arthritis Rheum.* **44** (1), 68–75 (2014).
6. Guler, M. A., Celik, O. F. & Ayhan, F. F. The important role of central sensitization in chronic musculoskeletal pain seen in different rheumatic diseases. *Clin. Rheumatol.* **39** (1), 269–274 (2020).
7. Kiltz, U., Baraliakos, X., Regel, A., Buhning, B. & Braun, J. Causes of pain in patients with axial spondyloarthritis. *Clin. Exp. Rheumatol.* **35** (Suppl 107(5)), 102–107 (2017).
8. Zhou, L. et al. Assessment of Neuropathic Pain in Ankylosing Spondylitis: prevalence and characteristics. *Pain Ther.* **10** (2), 1467–1479 (2021).
9. Ogdie, A. et al. Real-world patient experience on the path to diagnosis of Ankylosing Spondylitis. *Rheumatol. Therapy.* **6** (2), 255–267 (2019).
10. Sommer, C., Pan, Y., Blankfield, R. P., Kaelber, D. C. & Xu, R. Association of adverse cardiovascular events with gabapentin and Pregabalin among patients with fibromyalgia. *Plos One.* **19**(7), e0307515 (2024).
11. Smitha, K. A. et al. Resting state fMRI: a review on methods in resting state connectivity analysis and resting state networks. *Neuroradiol. J.* **30** (4), 305–317 (2017).
12. Cifre, I. et al. Disrupted functional connectivity of the pain network in fibromyalgia. *Psychosom. Med.* **74** (1), 55–62 (2012).
13. Stephan, K. E., Friston, K. J. & Frith, C. D. Dysconnection in schizophrenia: from abnormal synaptic plasticity to failures of self-monitoring. *Schizophr Bull.* **35** (3), 509–527 (2009).
14. Gursel, D. A. et al. Frontoparietal and salience network alterations in obsessive-compulsive disorder: insights from independent component and sliding time window analyses. *J. Psychiatry Neurosci.* **45** (3), 214–221 (2020).
15. Menon, V. Large-scale brain networks and psychopathology: a unifying triple network model. *Trends Cogn. Sci.* **15** (10), 483–506 (2011).
16. Smallwood, J. et al. The default mode network in cognition: a topographical perspective. *Nat. Rev. Neurosci.* **22** (8), 503–513 (2021).
17. Menon, V. & D'Esposito, M. The role of PFC networks in cognitive control and executive function. *Neuropsychopharmacology.* **47** (1), 90–103 (2022).
18. Napadow, V. et al. Intrinsic brain connectivity in fibromyalgia is associated with chronic pain intensity. *Arthritis Rheum.* **62** (8), 2545–2555 (2010).
19. Fallon, N., Chiu, Y., Nurmikko, T. & Stancak, A. Functional connectivity with the default Mode Network is altered in Fibromyalgia patients. *PLoS One.* **11** (7), e0159198 (2016).
20. Wu, Q., Inman, R. D. & Davis, K. D. Neuropathic pain in ankylosing spondylitis: a psychophysics and brain imaging study. *Arthritis Rheum.* **65** (6), 1494–1503 (2013).
21. Liu, Q. et al. Pain- and fatigue-related functional and structural changes in Ankylosing spondylitis: an fMRI Study. *Front. Med. (Lausanne).* **7**, 193 (2020).
22. Kim, H. et al. Fibromyalgia is characterized by altered frontal and cerebellar structural covariance brain networks. *Neuroimage Clin.* **7**, 667–677 (2015).
23. Schmidt-Wilcke, T. et al. Striatal grey matter increase in patients suffering from fibromyalgia—a voxel-based morphometry study. *Pain.* **132** (Suppl 1), S109–S116 (2007).
24. Mosch, B., Hagen, V., Herpertz, S. & Diers, M. Brain morphometric changes in fibromyalgia and the impact of psychometric and clinical factors: a volumetric and diffusion-tensor imaging study. *Arthritis Res. Ther.* **25** (1), 81 (2023).
25. Shi, H., Yuan, C., Dai, Z., Ma, H. & Sheng, L. Gray matter abnormalities associated with fibromyalgia: a meta-analysis of voxel-based morphometric studies. *Semin Arthritis Rheum.* **46** (3), 330–337 (2016).
26. Joel, S. E., Caffo, B. S., van Zijl, P. C. & Pekar, J. J. On the relationship between seed-based and ICA-based measures of functional connectivity. *Magn. Reson. Med.* **66** (3), 644–657 (2011).
27. Calhoun, V. D. & de Lacy, N. Ten key observations on the analysis of resting-state Functional MR Imaging Data Using Independent Component Analysis. *Neuroimaging Clin. N Am.* **27** (4), 561–579 (2017).

28. Douaud, G. et al. Anatomically related grey and white matter abnormalities in adolescent-onset schizophrenia. *Brain*. **130** (Pt 9), 2375–2386 (2007).
29. Wolfe, F. et al. 2016 revisions to the 2010/2011 fibromyalgia diagnostic criteria. *Semin Arthritis Rheum*. **46** (3), 319–329 (2016).
30. van der Linden, S., Valkenburg, H. A. & Cats, A. Evaluation of diagnostic criteria for ankylosing spondylitis. A proposal for modification of the New York criteria. *Arthritis Rheum*. **27** (4), 361–368 (1984).
31. Buysse, D. J., Reynolds, C. F. 3rd., Monk, T. H., Berman, S. R., & Kupfer, D. J. The Pittsburgh Sleep Quality Index: a new instrument for psychiatric practice and research. *Psychiatry Res*. **28** (2), 193–213 (1989).
32. Zigmond, A. S. & Snaith, R. P. The hospital anxiety and depression scale. *Acta Psychiatr Scand*. **67** (6), 361–370 (1983).
33. Krupp, L. B., LaRocca, N. G., Muir-Nash, J. & Steinberg, A. D. The fatigue severity scale. Application to patients with multiple sclerosis and systemic lupus erythematosus. *Arch. Neurol*. **46** (10), 1121–1123 (1989).
34. van Tubergen, A. et al. Assessment of fatigue in patients with ankylosing spondylitis: a psychometric analysis. *Arthritis Rheum*. **47** (1), 8–16 (2002).
35. Jenkinson, M., Bannister, P., Brady, M. & Smith, S. Improved optimization for the Robust and Accurate Linear Registration and Motion correction of brain images. *NeuroImage*. **17** (2), 825–841 (2002).
36. Bonda, E., Petrides, M., Ostry, D. & Evans, A. Specific involvement of human parietal systems and the amygdala in the perception of biological motion. *J. Neurosci*. **16** (11), 3737–3744 (1996).
37. Griffanti, L. et al. ICA-based artefact removal and accelerated fMRI acquisition for improved resting state network imaging. *Neuroimage*. **95**, 232–247 (2014).
38. Smith, S. M. et al. Correspondence of the brain's functional architecture during activation and rest. *Proc. Natl. Acad. Sci. U S A*. **106** (31), 13040–13045 (2009).
39. Soros, P. et al. Hyperactivity/restlessness is associated with increased functional connectivity in adults with ADHD: a dimensional analysis of resting state fMRI. *BMC Psychiatry*. **19** (1), 43 (2019).
40. Cui, Y. et al. Aberrant functional connectivity of default-mode network in type 2 diabetes patients. *Eur. Radiol*. **25** (11), 3238–3246 (2015).
41. Haber, S. N. Corticostriatal circuitry. *Dialogues Clin. Neurosci*. **18** (1), 7–21 (2016).
42. Grahn, J. A., Parkinson, J. A. & Owen, A. M. The cognitive functions of the caudate nucleus. *Prog Neurobiol*. **86** (3), 141–155 (2008).
43. Yuan, Z. et al. Altered functional connectivity of the right caudate nucleus in chronic migraine: a resting-state fMRI study. *J. Headache Pain*. **23** (1), 154 (2022).
44. Siemsen, B. M., Franco, D. & Lobo, M. K. Corticostriatal contributions to dysregulated motivated behaviors in stress, depression, and substance use disorders. *Neurosci. Res*. S0168-0102(22)00304-2 (2022).
45. Pizzagalli, D. A. et al. Reduced caudate and nucleus accumbens response to rewards in unmedicated individuals with major depressive disorder. *Am. J. Psychiatry*. **166** (6), 702–710 (2009).
46. Bluhm, R. et al. Resting state default-mode network connectivity in early depression using a seed region-of-interest analysis: decreased connectivity with caudate nucleus. *Psychiatry Clin. Neurosci*. **63** (6), 754–761 (2009).
47. Maletic, V. & Raison, C. L. Neurobiology of depression, fibromyalgia and neuropathic pain. *Front. Biosci. (Landmark Ed)*. **14** (14), 5291–5338 (2009).
48. Van Dyne, A. et al. Health, Psychological and demographic predictors of Depression in people with Fibromyalgia and Osteoarthritis. *Int. J. Environ. Res. Public Health*. **19**(6), 3413 (2022).
49. Fan, C. et al. Effects of meditation on neural responses to pain: a systematic review and meta-analysis of fMRI studies. *Neurosci. Biobehavioral Reviews*. **162**, 105735 (2024).
50. Almdahl, I. S., Martinussen, L. J., Agartz, I., Hugdahl, K. & Korsnes, M. S. Inhibition of emotions in healthy aging: age-related differences in brain network connectivity. *Brain Behav*. **11** (5), e02052 (2021).
51. Campbell, K. L., Grady, C. L., Ng, C. & Hasher, L. Age differences in the frontoparietal cognitive control network: implications for distractibility. *Neuropsychologia*. **50** (9), 2212–2223 (2012).
52. Pruitt, P. J., Tang, L., Hayes, J. M., Ofen, N. & Damoiseaux, J. S. Lifespan differences in background functional connectivity of core cognitive large-scale brain networks. *Neurosci. Res*. S0168-0102(22)00238-3 (2022).
53. Diaz-Piedra, C., Guzman, M. A., Buela-Casal, G. & Catena, A. The impact of fibromyalgia symptoms on brain morphometry. *Brain Imaging Behav*. **10** (4), 1184–1197 (2016).
54. Jensen, K. B. et al. Brain activations during pain. *Pain*. **157** (6), 1279–1286 (2016).
55. Xu, A. et al. Brain responses to noxious stimuli in patients with Chronic Pain. *JAMA Netw. Open*. **4**(1), e2032236 (2021).
56. Szabo, E. et al. Alterations in the structure and function of the brain in adolescents with new daily persistent headache: a pilot MRI study. *Headache: J. Head Face Pain*. **62** (7), 858–869 (2022).
57. Zhang, S. et al. Resting-State Functional Connectivity of the Cerebellum in Patients with Chronic Low Back Pain. *American Journal of Physical Medicine & Rehabilitation*. 2024.
58. Jones, G. T., Mallawaarachchi, B., Shim, J., Lock, J. & Macfarlane, G. J. The prevalence of fibromyalgia in axial spondyloarthritis. *Rheumatol. Int*. **40** (10), 1581–1591 (2020).

## Acknowledgements

We would like to extend our sincere gratitude to Professor Qingcong Kong for the counsel he provided for this study.

## Author contributions

D.L. made contributions to the design, data analysis and drafting of the manuscript. Y.Z. made contributions to the conception and design of this study. C.L. devised the acquisition parameters of the MRI scans and retrieved the fMRI data. J.Z., B.L. and M.Y. were in charge of the clinical assessments. O.J. and J.G. were the supervisors and oversaw this project. Funding was provided by J.G. All authors contributed to the editing of this manuscript.

## Funding

This work was supported by the grants from Guangdong Clinical Research Center of Immune disease (2020B1111170008); the Science and Technology Planning Project of Guangdong Province, China (2020B1515130005); National Key R&D Program of China (2021YFC2501306); Key-Area Research and Development Program of Guangdong Province (2023B1111030002).

## Declarations

### Ethics approval and consent to participate

This study was approved by the Research Ethics Board of the Third Affiliated Hospital of Sun Yat-sen University. Written informed consent was obtained from patients prior to the inclusion of this study according to the Declaration of Helsinki.

### Competing interests

The authors declare no competing interests.

### Additional information

**Correspondence** and requests for materials should be addressed to J.G. or O.J.

**Reprints and permissions information** is available at [www.nature.com/reprints](http://www.nature.com/reprints).

**Publisher's note** Springer Nature remains neutral with regard to jurisdictional claims in published maps and institutional affiliations.

**Open Access** This article is licensed under a Creative Commons Attribution-NonCommercial-NoDerivatives 4.0 International License, which permits any non-commercial use, sharing, distribution and reproduction in any medium or format, as long as you give appropriate credit to the original author(s) and the source, provide a link to the Creative Commons licence, and indicate if you modified the licensed material. You do not have permission under this licence to share adapted material derived from this article or parts of it. The images or other third party material in this article are included in the article's Creative Commons licence, unless indicated otherwise in a credit line to the material. If material is not included in the article's Creative Commons licence and your intended use is not permitted by statutory regulation or exceeds the permitted use, you will need to obtain permission directly from the copyright holder. To view a copy of this licence, visit <http://creativecommons.org/licenses/by-nc-nd/4.0/>.

© The Author(s) 2024